

Elliptic flow analysis with non-hydro mode in viscous hydrodynamics

Nikhil Hatwar* and M. Mishra†

Department of Physics, Birla Institute of Technology and Science, Pilani, Rajasthan, India

(Dated: February 2, 2022)

Hydrodynamics has been quite suitably used to model the thermal stage of the heavy-ion collision experiments especially in the low transverse momentum regime. But the satisfactory agreement of hydrodynamics for proton-proton collision has stirred up the discussions about the smallest volume for which the hydrodynamics can be applied. The meaning of hydrodynamics itself has been under scrutiny with non-requirement of local thermal equilibrium for its applicability. The second order viscous hydrodynamics requires a transport coefficient called relaxation time, which had to be included to avoid the causality violation in the system. This relaxation time controls the non-hydro mode in an out of equilibrium hydrodynamics theory. In phenomenological studies this relaxation time has been taken as a constant and much attention has gone into fixing shear viscosity to entropy density ratio, η/s . The dynamics of hydro and non-hydro modes govern the evolution of the system. In the present work, we study the effect of the variation of the relaxation times on the elliptic flow in Pb-Pb system, at $\sqrt{s_{NN}}=2.76$ TeV center-of-mass energy with optical Glauber and IPGlasma initial conditions. We find that this system operates throughout within the hydrodynamic regime. Non-hydro mode structure of the theory does not affect flow in the most central collisions and there is a noticeable increase in flow due to the initial state fluctuations.

I. INTRODUCTION

The fact that baryons have internal structure directly leads to the notion that a bulk medium of sub-nucleonic degrees of freedom is, in principle, possible. The energy density of at least a few GeV/fm³ is required to free up quarks from the nucleons [1]. The existence of such a medium was not very clear until the arrival of the Relativistic Heavy Ion Collider(RHIC) facility at Brookhaven National Laboratory where a deconfined state of sufficient time span was produced for observing the indirect unambiguous signatures of the Quark-Gluon Plasma(QGP). Strangeness enhancement [2] and elliptic flow [3] were among the preliminary indicators. The discovery of QGP in heavy ion collisions became more established with subsequent confirmation through other indicators like jet quenching and quarkonia suppression at RHIC. Efforts now are directed towards quantitatively fixing the boundaries of various regions of QCD phase diagram [4].

With the challenges involved in the theoretical development of the non-perturbation QCD dynamics, the progress in modelling these systems have been hindered. Moreover, deconfinement of quarks in QCD is still a unsolved problem [5]. Lattice QCD has been of some help in the QGP stage [6, 7], but we are far away from getting the whole system evolution under the roof of single dynamics. Thankfully, phenomenology has come for the rescue, allowing us to break the evolution into pre-equilibrium QGP and freeze-out stages. The use of hydrodynamics in modelling the transient QGP stage has been quite surprising [8], since traditionally hydrodynamics has been associated with the establishment of the local thermal

equilibrium of fluid of some kind.

However, hydrodynamics as an effective theory for explaining high energy collision has been evolved tremendously in the last two decades. Below we provide a very brief overview of the topics leading upto the present state of affairs. For an in-depth review of the topics, please lookup references [9–15].

Hydrodynamics is the collective dynamical evolution of a suitably sized bulk medium adhering to the system's symmetries. For the relativistic case, the conservation laws take the form, $\partial_\mu T^{\mu\nu} = 0$ for energy–momentum tensor and $\partial_\mu N^\mu = 0$ for conserved charge. The local values of temperature, $T(x)$, fluid velocity, $u_\mu(x)$ and chemical potential, $\mu(x)$ are the chosen hydrodynamic variables. The energy-momentum tensor can be decomposed as[16];

$$T^{\mu\nu} = \epsilon u^\mu u^\nu + P \Delta^{\mu\nu} + (w^\mu u^\nu + w^\nu u^\mu) + \Pi^{\mu\nu}. \quad (1)$$

Here, ϵ (energy density) and P (pressure) are scalar coefficients. w^μ represent transverse vector coefficient. $\Delta^{\mu\nu} \equiv g^{\mu\nu} + u^\mu u^\nu$ is the projector operator orthogonal to the fluid velocity, u^μ and $g^{\mu\nu}$ is the spacetime metric. The above expression without the $\Pi^{\mu\nu}$ term corresponds to 0th order ideal hydrodynamics. The $\Pi^{\mu\nu}$ tensor is introduced to account for the dissipative effects which is further decomposed as:

$$\Pi^{\mu\nu} = \pi^{\mu\nu} + \Delta^{\mu\nu} \Pi. \quad (2)$$

Π and $\pi^{\mu\nu}$ are the bulk and shear part of the viscous stress tensor. The form of the shear stress tensor, $\pi^{\mu\nu}$ and bulk pressure, Π are set up in accordance with the covariant form of the second law of thermodynamics[9]. When we set the expression for entropy 4–current as $s^\mu = s u^\mu$, where s is entropy density, we get;

$$\pi^{\mu\nu} = \eta \sigma^{\mu\nu} \quad \text{and} \quad \Pi = \zeta \partial_\mu u^\mu \quad (3)$$

* nikhil.hatwar@gmail.com

† madhukar@pilani.bits-pilani.ac.in

where η (shear viscosity) and ζ (bulk viscosity) are the transport coefficients. $\sigma^{\mu\nu}$ (shear tensor) is a traceless, transverse and symmetric tensor. This form of $\pi^{\mu\nu}$ and Π leads to the 1st order, Navier–Stokes theory. But when we introduce perturbations in energy density and fluid velocity, and evolve them, the diffusion speed obtained from the dispersion relation has a form which can increase arbitrarily. This theoretical formulation could not be considered as a satisfactory one, if it violates causality. It turns out that if the term $(-\tau_\pi u^\alpha \partial_\alpha \pi^{\mu\nu})$ is added in the expression of $\pi^{\mu\nu}$ above, the resulting diffusion speed stays below the speed of light. τ_π is another transport coefficient called as relaxation time. But this is still a make shift way to restore causality in the system.

Müller [17], Israel and Stewart [18, 19](MIS) suggested to modify the entropy 4–current expression employed above to include a term with viscous stress tensor¹. The entropy 4–current expression considered above was postulated for the fluid at equilibrium, which might not be the case for viscous QGP formed in the heavy ion collision. When we use this entropy 4–current in covariant 2nd law of thermodynamics, we obtain newer expressions² for $\pi^{\mu\nu}$ and Π . A perturbation analysis with these newer expressions lead an inherently causal system. There are a few variants of this theory [20], depending on how many terms are kept in $\pi^{\mu\nu}$ and Π . The viscous hydro code used for this study is based on MIS theory.

BRSSS theory[21] is a more comprehensive 2nd order viscous hydrodynamics. A bulk system is referred to have had *hydrodynamized* if the observables of collision show agreement with those of 2nd order hydrodynamics. A few 3rd order versions have also been worked up [22, 23]. A good 2nd order viscous hydro theory at the very least should reduce to the Navier–Stokes equation in the limit of long wavelengths, and must show causal signal propagation. One can also derive hydrodynamics from any microscopic theory e.g. kinetic theory or any QFT like QCD provided its dynamics show quasi-universality at large time scale [13]. The microscopic theory approach also helps in fixing the transport coefficients like ζ , η etc. [10].

The energy momentum tensor for such a theory in a non-equilibrium state is decomposed as;

$$T^{\mu\nu} = \langle T^{\hat{\mu}\hat{\nu}} \rangle_{eq} + \delta \langle T^{\hat{\mu}\hat{\nu}} \rangle \quad (4)$$

where the first term represents the equilibrium values of $T^{\mu\nu}$ and the second term account for the deviations from that equilibrium value. It is given under linear response theory as;

$$\delta \langle T^{\hat{\mu}\hat{\nu}} \rangle(x) = -\frac{1}{2} \int d^4y G_R^{\mu\nu, \alpha\beta}(x^0 - y^0, \mathbf{x} - \mathbf{y}) \delta g_{\alpha\beta}(y), \quad (5)$$

where, $G_R^{\mu\nu, \alpha\beta}(x^0 - y^0, \mathbf{x} - \mathbf{y})$ is the retarded 2–point correlator of $T^{\mu\nu}$. $\delta g_{\alpha\beta}(y)$ is the small perturbing term added to flat spacetime metric. This correlator when expressed in the Fourier space, $G_R^{\mu\nu, \alpha\beta}(\omega, \mathbf{k})$, has singularities in ω -plane. The \mathbf{k} is the momentum here and ω is given as;

$$\omega = \omega_h + i \omega_{nh} \quad (6)$$

where, ω_h is the excitation frequency for equilibrium plasma and is called a hydrodynamic mode. ω_{nh} is termed as transient mode or non-hydrodynamic mode frequency and is associated with the dissipative effects. The transient mode is responsible for disruption of the hydrodynamization process and is controlled with the *relaxation time* parameter which controls the duration for which viscous effects will remain active. The fact that hydrodynamics does not require local thermalization or even pressure isotropization to show agreement with the measurements [27], has become reasonable with the analysis of singularity structure of the underlying theory. An additional reason for the effectiveness of hydrodynamics especially in the phenomenological studies could be its late time universal behaviour from seemingly varied initial conditions [28].

Relativistic viscous hydrodynamics has been successfully used to explain experimental data obtained from the small collision system across various energies [24, 25]. This has led us to the question; What is the smallest size of the QGP droplet that can *hydrodynamize* [26]? To answer this we first need to ask, what is the singularity mode structure of the actual QCD dynamics producing QGP?

Alexi Kurkela et al., [29, 30] has performed a flow analysis with kinetic theory leading to MIS hydrodynamization, through a dimensionless physical quantity called opacity($\hat{\gamma}$) – a measure of transverse system size in units of the mean free path. They suggested that as opacity varies from 0 to 5, the system goes through a non-QGP (particle-like) stage to transition stage and to QGP(hydro-like) stage. Ulrich Heinz et al., [31] has emphasised on considering multiplicity rapidity density – dN/dy along with HBT radii to quantify the smallest QGP size. According to Romatschke [15], the large p_T regime of flow is due to non-hydro mode and this non-hydro mode can be studied through the relaxation time approach. He suggested that divergence of elliptic flow(v_2) for a deviation in relaxation times at low multiplicity could potentially indicate breakdown of the hydrodynamics.

In the present work, we study the response of the hydrodynamics on elliptic flow due to variation in the relaxation time with two initial conditions for Pb-Pb collision system at 2.76 TeV center of mass energy. In section.(II) we discuss details about the model starting with the viscous hydrodynamics we utilized. In subsection.(II A) we explain the parameters involved in model and the corresponding values which we used in our calculations. In subsection.(II B) we explain the optical Glauber and IP-

¹ see equation (39) of ref. [9]

² see equation (41) of ref. [9]

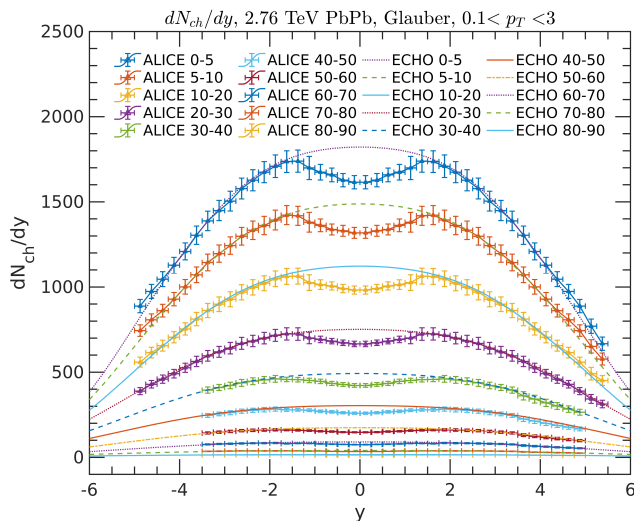


FIG. 1. Rapidity spectra of charged particles for 10 centrality classes. dN/dy from simulation are compared with ALICE pseudorapidity spectra, $dN/d\eta$ results[32].

Glasma initial conditions used in the viscous hydrodynamics. Subsection.(II C) has results for rapidity and transverse momentum spectra along with the hydrodynamic eccentricities. In section.(III), we present the results of elliptic flow as a function of transverse momentum and rapidity density. Finally, Section.(IV) describes the conclusions we derived from the results and possibility of the future outlook & improvement of this work.

II. METHODOLOGY

The second order viscous hydrodynamics used in this study is the ECHO-QGP [33, 34] – a publicly available code¹ based on the MIS theory. It could be used in either (2+1)-D or (3+1)-D settings. Spacetime evolution of all $T^{\mu\nu}$ components could be extracted at the output.

A tabular form of the lattice QCD Equation of State (EoS) by Wuppertal-Budapest collaboration [35] has been used in the present work. In this EoS, the energy density, speed of sound and pressure values are available only upto temperatures of 100 MeV. Hence we spline interpolated these with the corresponding quantities from Hadron Resonance Gas (HRG) [36] for lower temperature values and used the extended range as an input for hydrodynamics. The dissipative correction in the energy momentum tensor are introduced in ECHO-QGP as given in Eq.(2). The evolution of the shear part of the viscous

stress tensor is given by [33];

$$\pi^{\mu\nu} = -\eta \left(2\sigma^{\mu\nu} + \frac{4}{3} \frac{\tau_\pi}{\eta} d_\mu u^\mu \pi^{\mu\nu} + \frac{\tau_\pi}{\eta} \Delta_\alpha^\mu \Delta_\beta^\nu D \pi^{\alpha\beta} + \frac{\lambda_0}{\eta} \tau_\pi (\pi^{\mu\lambda} \Omega_\lambda^\nu + \pi^{\nu\lambda} \Omega_\lambda^\mu) \right). \quad (7)$$

Here, λ_0 is a scalar coefficient and Ω is a traceless, anti-symmetric, transverse vorticity tensor. d_μ is the covariant derivative given by $d_\mu u^\nu = \partial_\mu u^\nu + \Gamma_{\beta\mu}^\nu u^\beta$, where $\Gamma_{\beta\mu}^\nu$ are the Christoffel symbols. $D = u^\mu d_\mu$, is the comoving time derivative. The evolution of the bulk part of viscous stress tensor is given by;

$$\Pi = -\zeta \left(d_\mu u^\mu + \frac{\tau_\Pi}{\zeta} u^\alpha d_\alpha \Pi + \frac{4}{3} \frac{\tau_\Pi}{\zeta} \Pi d_\mu u^\mu \right). \quad (8)$$

The value of τ_Π , λ_0 , τ_π , η , ζ has to be provided for solving the above two equations. τ_Π is the bulk viscosity relaxation time, which represents how quickly the above 2^{nd} order form of bulk pressure relaxes to its leading-order form in Eq.(3). The above two equations are derived under the metric signature choice of $(-1, +1, +1, +1)$.

A. Input parameters

The form of relaxation time has been worked out for various microscopic approaches to viscous hydrodynamics viz. Boltzmann theory for relativistic limit [19, 38], weakly coupled QCD [39] and AdS/CFT [21, 40, 41]. In the ECHO-QGP, the relaxation time is introduced as;

$$\tau_\pi = \tau_{coe} \frac{\eta}{sT}, \quad (9)$$

where T is the temperature, τ_{coe} is the *coefficient* parameter in viscous hydrodynamics controlling the relaxation time. In SectionIII, the effect of the variation of this parameter has been studied. TableI shows the parameters used for 10 centralities of the Pb-Pb collision system. For Pb-Pb collision at 2.76 TeV, the hydrodynamic is initiated at $\tau_{start} = 0.2$ fm/c. The total inelastic nucleon-nucleon cross section is set at 61.8 mb for Pb-Pb hydrodynamics based on improved Monte Carlo Glauber analysis [42]. Initial hardness is a Glauber model parameter which was set at 0.2 [43]. Shear viscosity to entropy density ratio (η/s) is taken as a constant, 0.1 ($\approx 1.25 \times \frac{1}{4\pi}$)[1], which is above the KSS limit [44]. Relaxation time for bulk and shear viscosities is kept equal, $\tau_\pi = \tau_\Pi$ in hydrodynamics, but bulk viscosity has not been included for this study. The pseudo-critical temperature at which quarks to hadron phase transition occur, has been calculated by various lattice QCD collaborations and is a required parameter. It is set at 156 MeV[45]. Chemical freezeout is a point at which the inelastic scatterings cease between produced hadrons. This point is decided by the temperature, which in present model is fixed at 150 MeV[46].

¹ <http://theory.fi.infn.it/echoqgp/index.php>

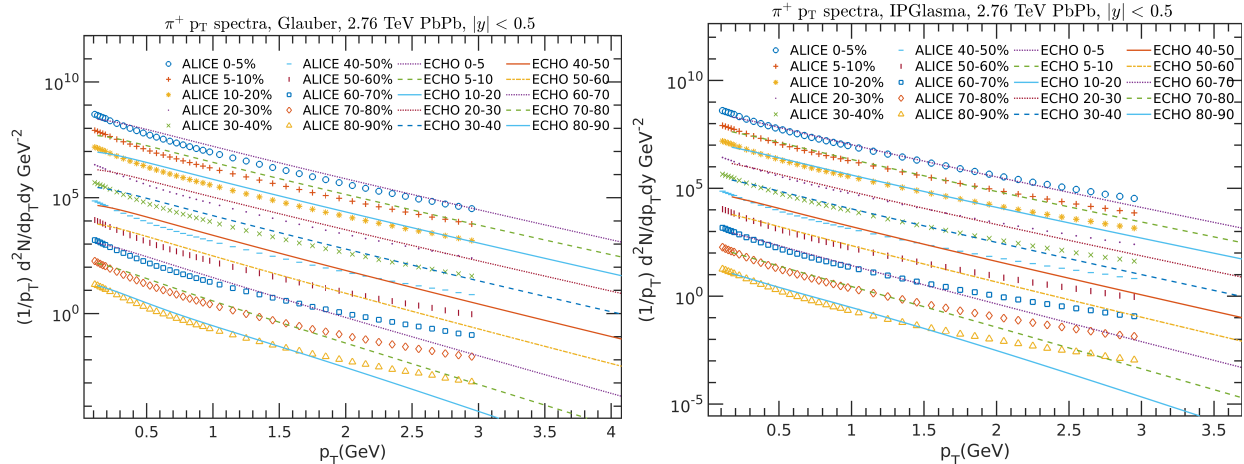


FIG. 2. Pion(π^+) p_T -spectra for geometric Glauber (left) and IPGlasma (right) compared with the corresponding ALICE results [37]. All values have been scaled up for better visibility.

B. Initial conditions

The elliptic flow analysis has been performed for two initial conditions viz. optical Glauber and IP-Glasma. In optical Glauber model, one assumes nucleons in the nucleus being distributed according to Wood-Saxon profile and having independent linear trajectories [47, 48]. Wood-Saxon distribution has a smooth plateau for nucleus which decays softly towards the edges. When two nuclei collide at some impact parameter, the number of participant's nucleon density is calculated using a simple relation² with the inelastic nucleon-nucleon cross section as input. The transverse distribution of participating

TABLE I. Centrality classes, impact parameter and initial energy density, ϵ_0 at ($\tau = t_{start}, x = 0, y = 0, \eta = 0$), that we used for the mentioned system of collisions. ϵ_0 was used only in 3D geometric Glauber initial condition. The energy density profile(fig.8) generated from IP-Glasma initial condition was scaled around the value of 0.2 for different centrality classes.

Pb-Pb at 2.76 TeV[42]		
cent(%)	b(fm)	ϵ_0
0-5	1.735	113
5-10	4.190	116
10-20	5.925	112
20-30	7.720	106
30-40	9.155	100
40-50	10.405	92
50-60	11.50	82
60-70	12.50	71
70-80	13.45	60
80-90	14.40	59

² eq.(8) of ref. [48]

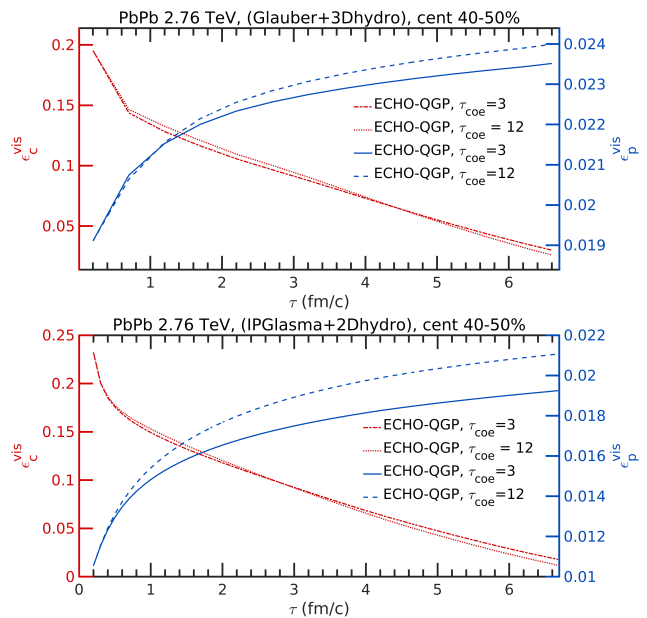


FIG. 3. Spatial and momentum eccentricity for the two mentioned initial conditions with different relaxation time parameters, τ_{coe} . The values start from $\tau_{start} = 0.2$ fm/c.

nucleons is then used to define the initial entropy/energy density for the hydrodynamic simulation.

IP-Glasma [49, 50] is the other initial condition, based on the Color Glass Condensate(CGC) framework which we have utilized³. The wavefunction of the high energy nuclei or hadron could be explained with an effective theory called CGC [51, 52]. The distribution of the nucleons

³ Public code at: <https://github.com/schenke/ipglasma>

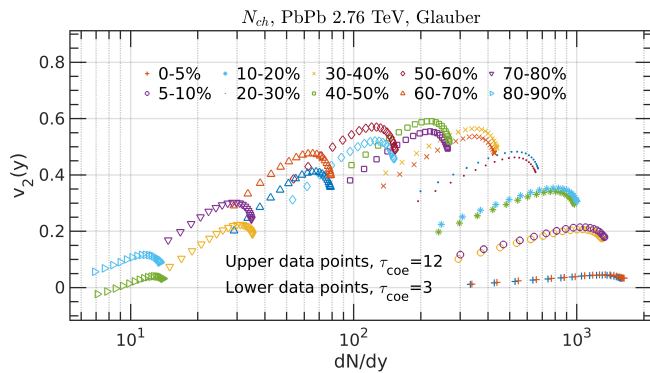


FIG. 4. Elliptic flow as a function of rapidity spectra for Glauber input condition to hydrodynamics.

in the nuclear wavefunction and the distribution of color charge inside nucleons are the key sources of initial state fluctuations. The Gaussian sampled color charges act as a source for gluon fields which are evolved using classical Yang-Mills equations[49].

Fig.(8) shows the initial energy density distribution from optical Glauber model and IPGlasma. We notice IPGlasma profile being extremely jagged and spiky, whereas Glauber initial condition is quite smooth. These two initial states encompass the two extreme limits of the initial state fluctuation viz. very high and very low spatial eccentricities. The initial state spatial eccentricity is proportional to the anisotropic flow calculated from momentum spectra of particles produced at freezeout. The initial energy density profile from IPGlasma is used as an input for (2+1)-D hydrodynamics run. Optical Glauber is run in (3+1)-D setting.

C. Spectra and Eccentricity

Fig.(1) shows the rapidity spectra of charged particles with Glauber initial condition for 10 centrality classes. The curves match satisfactorily with the experimental $dN/d\eta$ values for the extreme rapidities. For calculating quantities of charged particles, we have added the corresponding values for the pions($\pi^+ + \pi^-$), kaons($K^+ + K^-$) and protons($p^+ + p^-$) since these are abundantly produced species in the high energy collisions. This generated rapidity spectra was used to set the parameters related to the shape of initial energy density profile which is shown in the fig.(8) for Glauber model.

Fig.(2) shows the p_T spectra of pions(π^+) obtained with the two mentioned initial conditions along with the measured p_T spectra. We see a better match for IPGlasma. All the generated spectra comply to experimental values only in low p_T regime, where the hydrodynamic mode operates.

Momentum eccentricity is calculated in terms of $T^{\mu\nu}$

components as:

$$e_p \equiv \frac{\int d^2x_\perp (T^{xx} - T^{yy})}{\int d^2x_\perp (T^{xx} + T^{yy})} \quad (10)$$

ECHO-QGP calculates this quantity for ideal hydrodynamic case, which takes the form:

$$e_p \equiv \frac{\int d^2x_\perp (\epsilon + P) (u^x u^x - u^y u^y)}{\int d^2x_\perp [(\epsilon + P) (u^x u^x + u^y u^y) + 2P]} \quad (11)$$

We modified this formula for the viscous case i.e., by adding viscous component term, $(\pi^{xx} + \pi^{yy})$ to the integrand in both numerator and denominator in the above expression.

Fig.(3) shows spatial eccentricity(ϵ_c) and momentum eccentricity(ϵ_p) for the two mentioned initial conditions generated for $\tau_{coe} = 3$ and 12 at 40 – 50% centrality. We notice almost negligible to no effect on ϵ_c with respect to the variation in τ_{coe} , but ϵ_c starts are slightly larger value in IPGlasma than in Glauber model. For both initial conditions, ϵ_p starts at the same point and then diverge during the hydrodynamic evolution.

Below the pseudo-critical temperature, hadronic picture should emerge. In the model used here, particles of various species are assigned momentum according to Cooper–Frye scheme [54]. The resulting momentum spectra is then used to calculate the elliptic flow, $v_2 = \langle \cos[2(\phi - \Psi_{RP})] \rangle$, where Ψ_{RP} is the reaction plane angle which acts as a reference plane and ϕ is the transverse plane angle for a given particle with respect to the reaction plane.

III. FLOW RESULTS AND DISCUSSION

The collective flow measured by the experiments have a contribution from non-flow effects [55, 56]. In addition to this, flow-like signals could also be generated from parton-parton collision systems which are not associated with hydrodynamics e.g. parton escape mechanism [57]. These non-flow effects are difficult to eliminate especially in the higher flow harmonics where hydrodynamic flow itself is small. It is only the second harmonic coefficient–elliptic flow, which has an unambiguously significant contribution from hydrodynamic flow to indicate collectivity [58].

Hence, we study here the effect on elliptic flow due to the variation in the shear relaxation time, τ_π which controls the magnitude of the non-hydrodynamic mode of the QGP evolution. τ_π is controlled in the current model via τ_{coe} parameter as given in Eq.(9). τ_{coe} values have been studied for hydrodynamic limit of the microscopic theories like kinetic theory and AdS/CFT. It is usually set in the range of 2–6 fm/c [59]. The recent satisfactory application of the hydrodynamics in collision systems as small as p-p collision[25] has started the debate about figuring out the smallest size of QGP that can exist in the high energy nuclear collision. It has been suggested

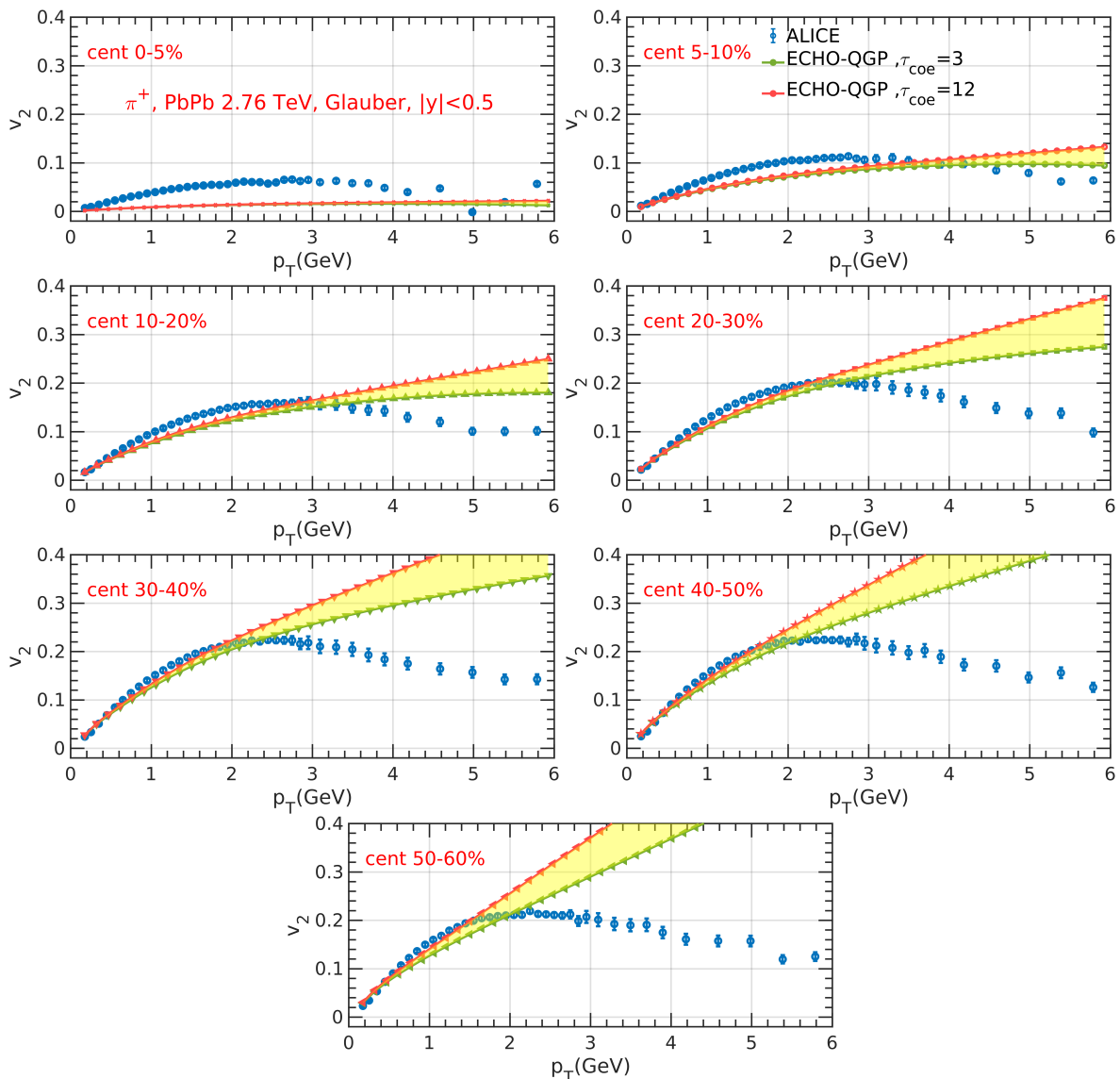


FIG. 5. Elliptic flow of pion(π^+) as a function of transverse momentum for 7 centrality classes obtained with optical Glauber input to hydrodynamics, along with the experimental results[53]

that an abrupt change in the elliptic flow for decreasing rapidity spectra due to the variation in the shear relaxation time could potentially indicate the break down of the hydrodynamics[27]. For doubling the value of τ_π , the charged particle's elliptic flow variation with rapidity density has suggested this break down to happen at $\frac{dN}{dy} \approx 2$, which is quite a small value. This could be the reason for the surprising success of the hydrodynamics in the high energy collisions. A modest maximum initial temperature reached in Pb-Pb collision at the LHC energy is around 600 MeV[60]. Using this temperature and $\eta/s = 0.1$ in Eq.(9), we get $\tau_\pi = \tau_{coe} \frac{\eta}{sT} = \tau_{coe} \frac{0.1}{600}$. In order to consider the effect of the variation in τ_π , we varied τ_{coe} in the range of 3 to 12, giving us $\tau_\pi = 0.098$ fm/c to 0.3946 fm/c.

In fig.(4), we plot elliptic flow of charged particles as a

function of rapidity spectra for Glauber initial condition. For IPGlasma, we could only generate average dN/dy around mid-rapidity at a given centrality as it is based on the (2+1)-D hydro system. But for Glauber case in Fig.(4), elliptic flow is plotted for all the centralities with full rapidity range. We see that the minimum elliptic flow occur at $dN/dy \approx 7$ and we don't see an abrupt change in elliptic flow at these dN/dy values. Therefore, according to the criteria stated above, even the most peripheral Pb-Pb collisions at $\sqrt{s_{NN}} = 2.76$ TeV are sufficiently hydrodynamic.

Fig.(5) shows the pion(π^+) elliptic flow as a function of the transverse momentum with increasing percent centrality classes or increasing impact parameter for a Glauber initial condition at the two values of τ_{coe} . For 0 – 5% centrality, no significant separation is seen

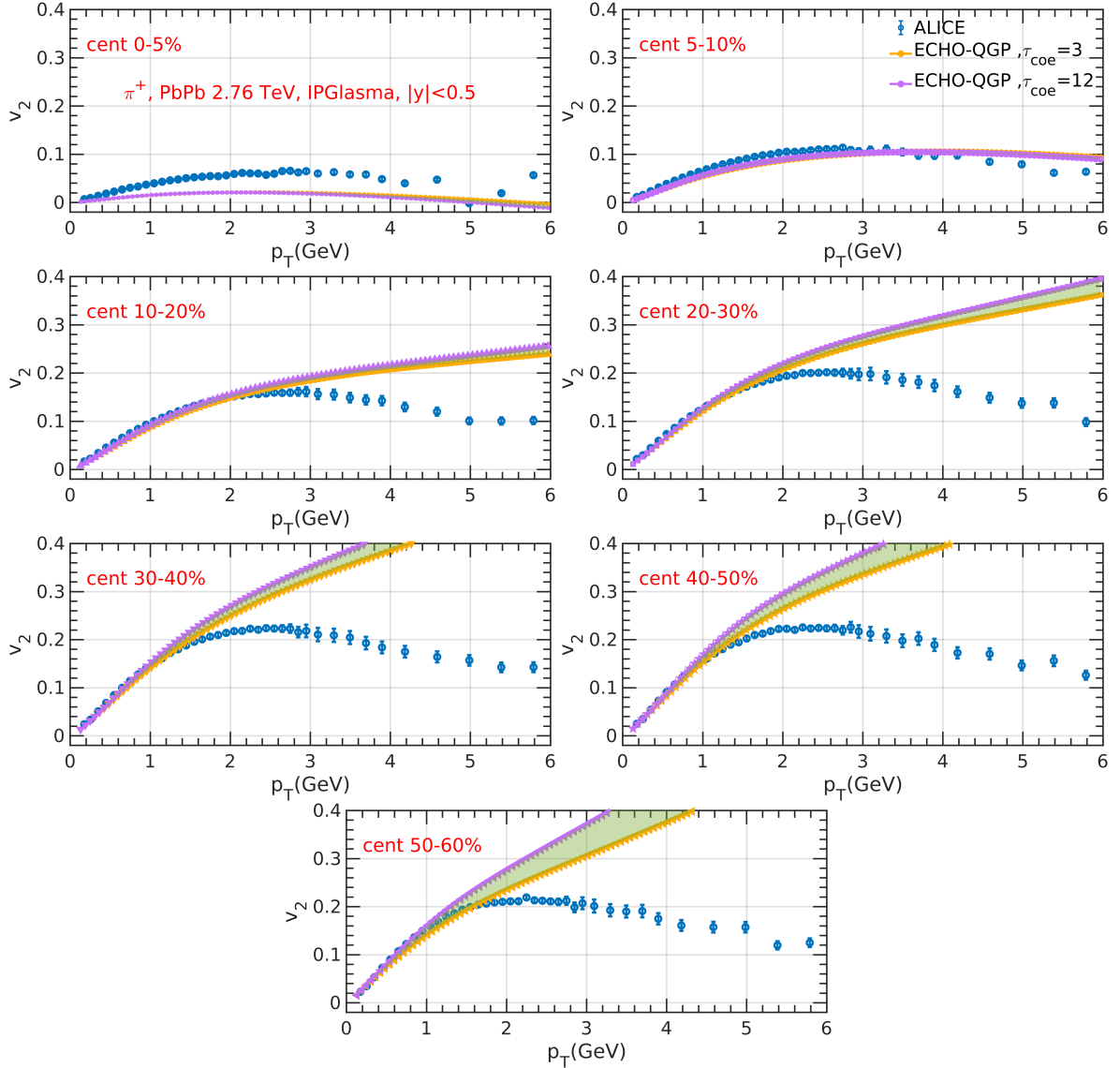


FIG. 6. Pion(π^+) elliptic flow as a function of transverse momentum for seven centrality classes obtained with IPGlasma input to hydrodynamics along with experimental elliptic flow results [53]. The shaded area represents the amount of increase in flow due to the use of larger relaxation time.

between curves of elliptic flow for $\tau_{coe} = 4, 12$ and the model predicts lesser flow than observed by the ALICE experiment. For increasing centrality classes, $\tau_{coe} = 3$ flow continue to under predict the experimental results and the separation between the elliptic flow curves for the two non-hydro mode curves increases monotonically. This is also apparent from the fact that the point where the two flow curves begin to diverge, shifts towards lower p_T values for increasing impact parameter.

Fig.(6) likewise shows the pions(π^+) elliptic flow with increasing centrality classes for IPGlasma initial condition. We also notice that for 0 – 5% and 5 – 10% centrality classes, there is not much separation between the curves of elliptic flow for the two τ_{coe} values.

We would also like to point out that for 0 – 5% central-

ity, the generated flow for (2+1)-D IPGlasma is slightly larger when compared to the same in (3+1)-D Glauber plot. To confirm this, we have plotted flow from Glauber and IPGlasma initial conditions on the same plot in Fig.(7). We suspected that this increased flow could also have been due to the changing dynamics from 2D to 3D. Hence, we have also shown elliptic flow for (2+1)-D Glauber case in Fig.(7). (3+1)-D case does produce slightly more flow than (2+1)-D case, but the flow from IPGlasma is still larger than even (3+1)-D hydro case. This subtle increase could only be a result of initial state fluctuation in the spatial eccentricity, which is larger in IPGlasma model. A study about smoothing of initial state has been carried out [61], but no noticeable change in the flow harmonics was found.

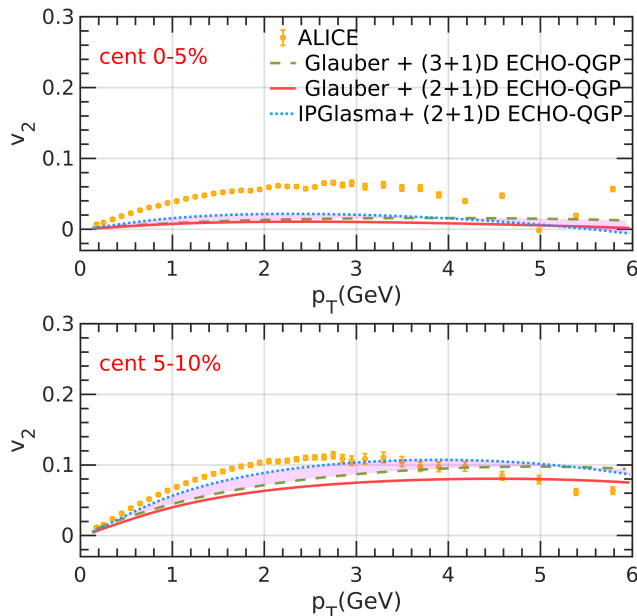


FIG. 7. Pion(π^+) elliptic flow as a function of transverse momentum for $\tau_{coe} = 3$. The shaded area represents the difference in flow between 2-D IPGlasma and 3-D Glauber model. This comparison is meaningful only for low impact parameter centrality classes, where the separation between elliptic flow for the two τ_{coe} values overlaps, atleast for $p_T < 3$ GeV/c.

The measured elliptic flow in the experiments has contribution from hydrodynamic flow which is decided by the dynamics of hydro and non-hydro modes in the QGP stage. Various non-flow effects at various multiplicity also contribute to flow measurement. In addition, event-by-event fluctuations in the flow also exists.

Non-flow contribution arises due to the effects like partonic bremsstrahlung, fragmentation of jet and dijets, resonance decay etc, which are local in nature.

Various studies have been carried out to explain the total measured flow. But the models differ in size of fluctuation, non-flow, relaxation times and *number of terms in 2nd order gradient expansion*. However, the hydrodynamic flow is the quantity of our interest, which provides the true properties of the medium. For this, not just elimination of other flow contributors, but their quantification is required as a function of centrality and multiplicity across various collision systems.

The non-hydrodynamic mode is a theoretical artifact of 2nd order hydrodynamics which controls when will system stop showing hydrodynamic behaviour. Hence, for both initial conditions, we see, $\tau_{coe}=12$ flow curve is steeply increasing when compared with the $\tau_{coe}=3$ curve. But, for IPGlasma, we see lesser shaded region than the Glauber case suggesting weaker non-hydro mode in IPGlasma system. We also see that the effect of non-hydro mode is almost none to negligible in the most central collisions and increases when we move towards non-central collision. This could mean that the strength of "hy-

dro mode" contribution to the flow reduces with increasing impact parameter. Hence, phenomenological studies should be cautious of the effect of non-hydro mode structure at the intermediate transverse momentum regime viz., 1 – 3 GeV/c, especially at the peripheral collision where strength of non-hydro mode is quite significant. We also find that the flow from IPGlasma initial condition to be in better agreement with the experimental results than the optical Glauber model.

IV. CONCLUSION AND OUTLOOK

In this study we analysed the elliptic flow arising out of a 2nd order viscous hydrodynamic system based on MIS theory. The system under consideration is Pb-Pb collision at $\sqrt{s_{NN}} = 2.76$ TeV center of mass LHC energy. We made use of two initial conditions viz., IPGlasma and optical Glauber model to account for the maximum variation in the initial state fluctuations. The role of the hadron rescattering in the flow has been neglected in this study. Rapidity and transverse momentum spectra has been reproduced, along with initial spatial and momentum eccentricity to constrain the model parameters. We varied the 2nd order transport coefficient of the theory corresponding to the shear viscosity termed as relaxation time to see its effect on the elliptic flow as a function of the transverse momentum and rapidity spectra. The results were compared with the corresponding experimental values obtained from the ALICE experiment at LHC. Based on the results obtained, following inferences (and questions) can be drawn (raised):

- Even the most peripheral PbPb, 2.76 TeV collisions that could be quantified within the experimentally measured centrality classes are within the hydrodynamic regime based on presently agreed upon criteria [27, 31].
- Larger relaxation time causes larger elliptic flow in the viscous hydrodynamic theory. We see a larger flow increment in the Glauber model than in IPGlasma model. (Could this mean that the non-hydrodynamic mode is sensitive to the initial state fluctuation?)
- Elliptic flow in the most central collisions is not affected by the non-hydro mode structure of the theory. For increasing impact parameter, the non-hydro mode participation also increases. (Hence, could we compare flow from different models at the most central collisions without worrying about non-hydro mode structure of the theory? The only caveat being the total flow itself is quite small in the most central collisions.)
- Initial state fluctuations have a noticeable effect on the elliptic flow and could even be quantifiable with a more comprehensive study.

In the upcoming work, we would like to extend this study for collision systems at RHIC energies. The IPGlasma initial condition used was a 2-dimensional model. That is why we had to use (2+1)-dimensional viscous hydrodynamics with it. An obvious improvement one could think of is switching to a 3-D IPGlasma initial condition [62]. Moreover, one could also use the complete energy momentum tensor from the initial condition instead of just the initial energy density [63]. Bulk viscosity has been kept zero in this study. But it does play significant role in evolution [64]. The relaxation times for bulk viscosity could be independently analysed in a similar way.

ACKNOWLEDGMENTS

We are thankful to Gabriele Inghirami for clearing our doubts and helping at numerous times in using the viscous hydrodynamics code. We are also grateful to Chun

Shen, Paul Romatschke and Rajeev Bhalerao for clearing our doubts about flow. Nikhil Hatwar would like to thank BITS-Pilani for the financial support.

Appendix A: Initial energy density profile and parameter setting

Fig.(9) shows rapidity spectra normalized to N_{part} as a function of N_{part} . The value of maximum energy density has to be set in for Glauber initial condition. One can adjust this value for a given centrality such that the p_T spectra curve matches with the corresponding experimental results. But the p_T spectra curves span a wide range of values. Hence, we made use of $(dN/dy)/(N_{part}/2)$ vs N_{part} results to set the initial energy density profile for Glauber model and scaling of energy density profile in IPGlasma model. The dN/dy results from ECHO-QGP had to be scaled up by a factor of 4 and 5 for pions and charged particles, respectively to match with the corresponding experimental results.

-
- [1] W. Busza, K. Rajagopal, and W. Van Der Schee, Heavy ion collisions: the big picture and the big questions, *Annual Review of Nuclear and Particle Science* **68**, 339 (2018).
 - [2] J. Letessier and J. Rafelski, Observing quark-gluon plasma with strange hadrons, *International Journal of Modern Physics E* **9**, 107 (2000).
 - [3] K. Ackermann, N. Adams, C. Adler, Z. Ahammed, S. Ahmad, C. Allgower, J. Amsbaugh, M. Anderson, E. Andersen, H. Arnesen, *et al.*, Elliptic Flow in Au+Au Collisions at $\sqrt{s_{NN}}=130$ GeV, *Physical Review Letters* **86**, 402 (2001).
 - [4] G. Odyniec, The RHIC beam energy scan program in STAR and what's next . . . , *Journal of Physics: Conference Series* **455**, 012037 (2013).
 - [5] T.-Y. Wu and P. W. Hwang, *Relativistic quantum mechanics and quantum fields* (World Scientific Publishing Company, 1991).
 - [6] C. Ratti, Lattice qcd and heavy ion collisions: a review of recent progress, *Reports on Progress in Physics* **81**, 084301 (2018).
 - [7] A. Bazavov, T. Bhattacharya, C. DeTar, H.-T. Ding, S. Gottlieb, R. Gupta, P. Hegde, U. Heller, F. Karsch, E. Laermann, *et al.*, Equation of state in (2+1)-flavor qcd, *Physical Review D* **90**, 094503 (2014).
 - [8] M. Luzum and P. Romatschke, Conformal relativistic viscous hydrodynamics: Applications to rhic results at $\sqrt{s_{NN}}=200$ gev, *Physical Review C* **78**, 034915 (2008).
 - [9] P. Romatschke, New developments in relativistic viscous hydrodynamics (2010).
 - [10] P. Kovtun, Lectures on hydrodynamic fluctuations in relativistic theories (2012).
 - [11] S. Jeon and U. Heinz, Introduction to hydrodynamics (2016).
 - [12] A. Jaiswal and V. Roy, Relativistic hydrodynamics in heavy-ion collisions: general aspects and recent developments (2016).
 - [13] W. Florkowski, M. P. Heller, and M. Spaliński, New theories of relativistic hydrodynamics in the lhc era (2018).
 - [14] J.-P. Blaizot and L. Yan, Emergence of hydrodynamical behavior in expanding ultra-relativistic plasmas (2020).
 - [15] P. Romatschke, Do nuclear collisions create a locally equilibrated quark-gluon plasma?, *The European Physical Journal C* **77**, 1 (2017).
 - [16] C. Eckart, The thermodynamics of irreversible processes. iii. relativistic theory of the simple fluid, *Phys. Rev.* **58**, 919 (1940).
 - [17] I. Müller, Zum paradoxon der wärmeleitungstheorie, *Zeitschrift für Physik* **198**, 329 (1967).
 - [18] W. Israel, Nonstationary irreversible thermodynamics: a causal relativistic theory, *Annals of Physics* **100**, 310 (1976).
 - [19] W. Israel and J. M. Stewart, Transient relativistic thermodynamics and kinetic theory, *Annals of Physics* **118**, 341 (1979).
 - [20] G. S. Denicol, T. Koide, and D. H. Rischke, Dissipative relativistic fluid dynamics: A new way to derive the equations of motion from kinetic theory, *Phys. Rev. Lett.* **105**, 162501 (2010).
 - [21] R. Baier, P. Romatschke, D. T. Son, A. O. Starinets, and M. A. Stephanov, Relativistic viscous hydrodynamics, conformal invariance, and holography, *Journal of High Energy Physics* **2008**, 100 (2008).
 - [22] A. Jaiswal, Relativistic third-order dissipative fluid dynamics from kinetic theory, *Phys. Rev. C* **88**, 021903 (2013).
 - [23] S. M. Diles, L. A. Mamani, A. S. Miranda, and V. T. Zanchin, Third-order relativistic hydrodynamics: dispersion relations and transport coefficients of a dual plasma, *Journal of High Energy Physics* **2020**, 1 (2020).
 - [24] B. Schenke, C. Shen, and P. Tribedy, Running the gamut of high energy nuclear collisions, *Physical Review C* **102**,

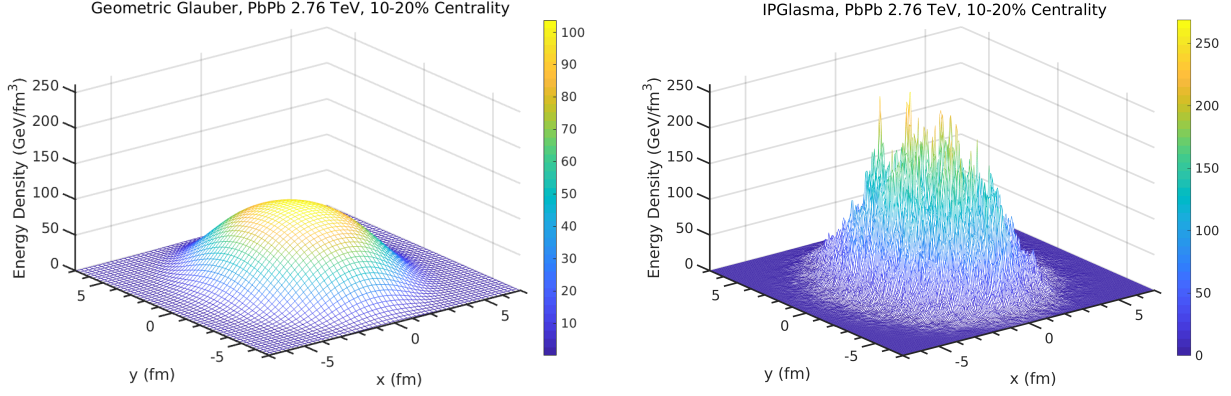


FIG. 8. Energy density distribution in the transverse plane, ($x = 0, y = 0, \text{rapidity} = 0, \tau = 0.2 \text{ fm}/c$), for optical Glauber model(left) and IP-Glasma(right) initial condition for 10-20% centrality class.

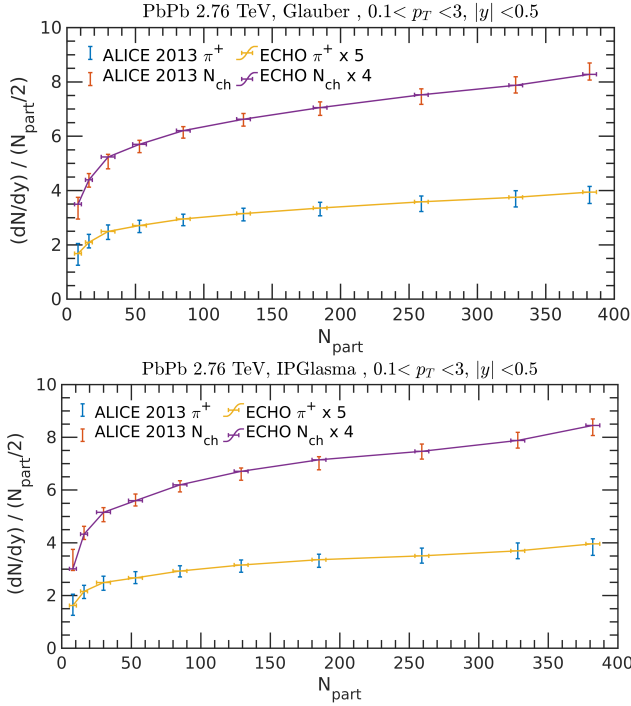


FIG. 9. Rapidity spectra normalized to number of participants(N_{part}) as a function of N_{part} for optical Glauber(above) and IPGlasma(below) initial conditions.

- 044905 (2020).
- [25] M. Habich, G. Miller, P. Romatschke, and W. Xiang, Testing hydrodynamic descriptions of p+p collisions at $\sqrt{s} = 7 \text{ tev}$, *The European Physical Journal C* **76**, 1 (2016).
- [26] J. L. Nagle and W. A. Zajc, Small system collectivity in relativistic hadronic and nuclear collisions, *Annual Review of Nuclear and Particle Science* **68**, 211 (2018).
- [27] P. Romatschke, Do nuclear collisions create a locally equilibrated quark-gluon plasma?, *The European Physical*

- Journal C* **77**, 1 (2017).
- [28] P. Castorina, A. Iorio, D. Lanteri, H. Satz, and M. Spusta, Universality in hadronic and nuclear collisions at high energy, *Phys. Rev. C* **101**, 054902 (2020).
- [29] A. Kurkela, U. A. Wiedemann, and B. Wu, Flow in aa and pa as an interplay of fluid-like and non-fluid like excitations, *The European Physical Journal C* **79**, 1 (2019).
- [30] A. Kurkela, U. A. Wiedemann, and B. Wu, Opacity dependence of elliptic flow in kinetic theory, *The European Physical Journal C* **79**, 1 (2019).
- [31] U. Heinz and J. S. Moreland, Hydrodynamic flow in small systems or: “how the heck is it possible that a system emitting only a dozen particles can be described by fluid dynamics?”, in *Journal of Physics: Conference Series*, Vol. 1271 (IOP Publishing, 2019) p. 012018.
- [32] J. Adam, D. Adamova, M. Aggarwal, G. A. Rinella, M. Agnello, N. Agrawal, Z. Ahammed, S. Ahn, S. Aiola, A. Akimov, *et al.*, Centrality evolution of the charged-particle pseudorapidity density over a broad pseudorapidity range in Pb-Pb collisions at $\sqrt{s_{NN}} = 2.76 \text{ TeV}$, *Physics Letters B* **754**, 373 (2016).
- [33] L. Del Zanna, V. Chandra, G. Inghirami, V. Rolando, A. Beraudo, A. De Pace, G. Pagliara, A. Drago, and F. Becattini, Relativistic viscous hydrodynamics for heavy-ion collisions with echo-ggp, *The European Physical Journal C* **73**, 1 (2013).
- [34] V. Rolando, G. Inghirami, A. Beraudo, L. Del Zanna, F. Becattini, V. Chandra, A. De Pace, and M. Nardi, Heavy ion collision evolution modeling with echo-ggp, *Nuclear Physics A* **931**, 970 (2014).
- [35] S. Borsanyi, G. Endrődi, Z. Fodor, A. Jakovac, S. D. Katz, S. Krieg, C. Ratti, and K. K. Szabo, The qcd equation of state with dynamical quarks, *Journal of High Energy Physics* **2010**, 1 (2010).
- [36] S. Chatterjee, R. M. Godbole, and S. Gupta, Stabilizing hadron resonance gas models, *Phys. Rev. C* **81**, 044907 (2010).
- [37] J. Adam, Adagmar, M. M. Aggarwal, G. A. Rinella, M. Agnello, N. Agrawal, Z. Ahammed, S. U. Ahn, I. Aimo, S. Aiola, *et al.*, Centrality dependence of the nuclear modification factor of charged pions, kaons, and protons in Pb-Pb collisions at $\sqrt{s_{NN}} = 2.76 \text{ TeV}$, *Physical Review C* **93**, 034913 (2016).

- [38] R. Baier, P. Romatschke, and U. A. Wiedemann, Dissipative hydrodynamics and heavy-ion collisions, *Phys. Rev. C* **73**, 064903 (2006).
- [39] M. A. York and G. D. Moore, Second order hydrodynamic coefficients from kinetic theory, *Phys. Rev. D* **79**, 054011 (2009).
- [40] M. P. Heller and R. A. Janik, Viscous hydrodynamics relaxation time from ads/cft correspondence, *Phys. Rev. D* **76**, 025027 (2007).
- [41] S. Bhattacharyya, R. Loganayagam, I. Mandal, S. Minwalla, and A. Sharma, Conformal nonlinear fluid dynamics from gravity in arbitrary dimensions, *Journal of High Energy Physics* **2008**, 116 (2008).
- [42] C. Loizides, J. Kamin, and D. d’Enterria, Improved monte carlo glauber predictions at present and future nuclear colliders, *Phys. Rev. C* **97**, 054910 (2018).
- [43] D. d’Enterria and C. Loizides, Progress in the glauber model at collider energies, *Annual Review of Nuclear and Particle Science* **71**, 315 (2021).
- [44] P. K. Kovtun, D. T. Son, and A. O. Starinets, Viscosity in strongly interacting quantum field theories from black hole physics, *Phys. Rev. Lett.* **94**, 111601 (2005).
- [45] H.-T. Ding, New developments in lattice qcd on equilibrium physics and phase diagram, *Nuclear Physics A* **1005**, 121940 (2021).
- [46] A. Mazeliauskas and V. Vislavicius, Temperature and fluid velocity on the freeze-out surface from π , K , and p spectra in pp , p -Pb, and Pb-Pb collisions, *Phys. Rev. C* **101**, 014910 (2020).
- [47] P. F. Kolb, U. Heinz, P. Huovinen, K. J. Eskola, and K. Tuominen, Centrality dependence of multiplicity, transverse energy, and elliptic flow from hydrodynamics, *Nuclear Physics A* **696**, 197 (2001).
- [48] M. L. Miller, K. Reygers, S. J. Sanders, and P. Steinberg, Glauber modeling in high-energy nuclear collisions (2007).
- [49] B. Schenke, P. Tribedy, and R. Venugopalan, Fluctuating glasma initial conditions and flow in heavy ion collisions, *Physical Review Letters* **108**, 252301 (2012).
- [50] B. Schenke, P. Tribedy, and R. Venugopalan, Event-by-event gluon multiplicity, energy density, and eccentricities in ultrarelativistic heavy-ion collisions, *Phys. Rev. C* **86**, 034908 (2012).
- [51] L. McLerran and R. Venugopalan, Computing quark and gluon distribution functions for very large nuclei, *Phys. Rev. D* **49**, 2233 (1994).
- [52] F. Gelis, E. Iancu, J. Jalilian-Marian, and R. Venugopalan, The color glass condensate, *Annual Review of Nuclear and Particle Science* **60**, 463 (2010).
- [53] B. Abelev, J. M. Adam, M. Agnello, A. Agostinelli, N. Agrawal, Z. Ahammed, N. Ahmad, I. Ahmed, *et al.*, Elliptic flow of identified hadrons in Pb-Pb collisions at $\sqrt{s_{NN}} = 2.76$ TeV, *Journal of High Energy Physics* **2015**, 1 (2015).
- [54] F. Cooper and G. Frye, Single-particle distribution in the hydrodynamic and statistical thermodynamic models of multiparticle production, *Phys. Rev. D* **10**, 186 (1974).
- [55] R. Snellings, Elliptic flow: a brief review, *New Journal of Physics* **13**, 055008 (2011).
- [56] J. Jia and S. Mohapatra, Disentangling flow and nonflow correlations via bayesian unfolding of the event-by-event distributions of harmonic coefficients in ultrarelativistic heavy-ion collisions, *Phys. Rev. C* **88**, 014907 (2013).
- [57] L. He, T. Edmonds, Z.-W. Lin, F. Liu, D. Molnar, and F. Wang, Anisotropic parton escape is the dominant source of azimuthal anisotropy in transport models, *Physics Letters B* **753**, 506 (2016).
- [58] P. Romatschke, Collective flow without hydrodynamics: simulation results for relativistic ion collisions, *The European Physical Journal C* **75**, 1 (2015).
- [59] H. Song and U. Heinz, Interplay of shear and bulk viscosity in generating flow in heavy-ion collisions, *Phys. Rev. C* **81**, 024905 (2010).
- [60] M. Alqahtani, M. Nopoush, R. Ryblewski, and M. Strickland, (3 + 1)D quasiparticle anisotropic hydrodynamics for ultrarelativistic heavy-ion collisions, *Phys. Rev. Lett.* **119**, 042301 (2017).
- [61] J. Noronha-Hostler, J. Noronha, and M. Gyulassy, Sensitivity of flow harmonics to subnucleon scale fluctuations in heavy ion collisions, *Phys. Rev. C* **93**, 024909 (2016).
- [62] B. Schenke and S. Schlichting, 3d glasma initial state for relativistic heavy ion collisions, *Phys. Rev. C* **94**, 044907 (2016).
- [63] C. Chattopadhyay, R. S. Bhalerao, J.-Y. Ollitrault, and S. Pal, Effects of initial-state dynamics on collective flow within a coupled transport and viscous hydrodynamic approach, *Phys. Rev. C* **97**, 034915 (2018).
- [64] S. Ryu, J.-F. Paquet, C. Shen, G. Denicol, B. Schenke, S. Jeon, and C. Gale, Importance of the bulk viscosity of qcd in ultrarelativistic heavy-ion collisions, *Physical review letters* **115**, 132301 (2015).